AIMS Mathematics, 10(12): 28689–28713.
DOI: 10.3934/math.20251263
Received: 16 August 2025
Revised: 22 October 2025
Accepted: 28 October 2025
Published: 04 December 2025

http://www.aimspress.com/journal/Math

Research article

Analytical soliton solutions and dynamical behavior of a conformable fractional nonlinear system with Hamiltonian structure

Maher Alwuthaynani*

Department of Mathematics, College of Alkhormah, Taif University, Taif University, Saudi Arabia

* **Correspondence:** Email: m.alwuthaynani@tu.edu.sa.

Abstract: This paper focuses on solving the precise wave solution and dynamics properties, as well as stability in a nonlinear system in space-time in terms of conformable fractional derivatives. The generalized Riccati-Bernoulli sub-ODE method along with Bäcklund transformation of analyzing the underlying model captures key nonlinear dynamics that are of interest in contemporary engineering, physics, and applied mathematics. Using a conformable fractional derivative operator we have made a leap beyond classical models in integer orders to be able to represent more realistic aspects of the effects of memory and heredity both on the complex media. We have obtained the solutions and they include new types of dark kink solitons whose propagations correspond to localized transitions between two different states of medium. The qualitative character of these solutions can be visualized by 2D profiles with different values of the fractional-order parameter (α) and 3D plots in the classical case. The influence of the changes in the fractional ordering on the amplitude of the waves and stability of the solitons is explained with the help of these graphical representations. Moreover, a section of the phase-space and bifurcation diagrams related to the associated planar dynamical system emphasize the sensitivity and abundance of dynamics of the model with respect to parameter perturbation. This multifaceted research enriches the knowledge about nonlinear wave propagation in multi-complex media, as well as providing insights of relevance into the dynamics and relationships between nonlinearity, dispersion, and fractional-order dynamics.

Keywords: magneto-electro-elastic (MEE) circular rod; bifurcation and stability analysis; generalized Riccati-Bernoulli sub-ODE method; Bäcklund tranformation; solitons
Mathematics Subject Classification: 34G20, 35A20, 35A22, 35R11

1. Introduction

Magneto-electro-elastic (MEE) materials, over the past few years, have turned out to be powerful multi-functional composites with an essential key role in a wide range of fields of nano-technology and micro-scale engineering. Researchers have been able to combine these magnetostrictive, piezoelectric, ferroelectric, dielectric, and elastic properties with nonlinear and frequency-dependent response with the advantage of making them preferred candidates of advanced energy harvesting, thermal stability, and smart sensing applications. These versatile materials allow the unobtrusive hybridization of magnetic, electric, and mechanical fields and would therefore allow the creation of advanced sensors, actuators, and transducers that can form part of the advanced technologies in aerospace, robotics, biomedical, and telecommunication systems. The study of waves propagation in MEE media, especially the study of longitudinal waves, e.g., sound, seismic, ultrasonic waves traveling in MEE circular rods, gives an important insight into the optimization of the performance of the device as well as the design of materials. The progress of technologies in the realms of biomechanics, meteorology, musical acoustics, and signal transmission is directly influenced by these studies. Though nonlinear mathematical modeling is widely used among several tools developed to study the behavior of MEE structures, even though a wide range of approaches have been adopted to examine the same in a more realistic manner, still nonlinear mathematical modeling remains one of the most efficient and accurate tools to consider the complex nature of the coupled systems [1–4].

Nonlinear partial differential equations (NLPDEs) are used as basic modeling tools to describe a broad range of complicated phenomena in the natural sciences. These PDEs are frequently reduced to nonlinear evolution equations (NLEEs) under appropriate perturbation methods, and these equations carry the spirit of dynamics and governing laws of diverse physical, biological, and engineering systems. The existence of the exact or approximate mathematical solutions to these equations has attracted much attention of the scientific community since the analytical solutions are of great help in perceiving the mechanisms underlying the phenomenon being tentatively modeled [5–10]. Various computational and symbolic techniques have been devised and perfected over the past few decades to find the closed-form solutions of these nonlinear models and hence enable the researchers to better understand, predict, and manipulate the real-life models represented by NLPDEs. Multiple investigators within the NLPDE domain have generated many advanced approaches to find soliton solutions. Researchers employ various solution methods such as the new extended direct algebraic method [11] the Sardar sub-equation scheme [12, 13] the fractional evolution process [14] the general algebraic scheme [15] the unified method [16, 17] the improved Kudryashov technique [18, 19] the adapted (G'/G)-expansion scheme [20] and so on [21–25].

Fractional calculus is a powerful mathematical theory based on enriching the basic principles of classical calculus with concepts of integration and differentiation of any order. The history of fractional operators began early in the emergence of classical calculus, when in a 1695 letter between G.W. Leibniz and Marquis de Hopital, the author speculated on the possibility of such an operator containing a complex meaning. Since that period, it has attracted the attention of many and several prominent mathematicians such as Euler, Liouville, Laplace, Riemann, and Letnikov. Since the 19th century, fractional calculus experienced significant theoretical growth, which later became the mathematics of new disciplines that include fractional differential equations, fractional geometry, and fractional dynamics [26]. Fractional calculus has recently gained increased significance due to its potential to

explain memory and hereditary features in the character of many physical and biological processes that cannot be fully accounted for by integer-order models. Consequently, fractional derivatives and integrals have become a common tool in a variety of scientific and engineering fields, such as viscoelasticity, control theory, signal processing, bioengineering, fluid mechanics, and the anomalous diffusion processes. Its significance keeps growing as more scientists use fractional-order models to better understand complex real systems.

Here, we are concerned with the fractional modeling and solution of longitudinal propagation of waves in magneto-electro-elastic (MEE) circular rods. These materials have a coupled mechanical, electrical, and magnetic behavior, and hence their applications could be used in multi-functional devices like sensors, actuators, and transducers in aerospace, robotics, and biomedical systems. The conduction of the wave by the MEE rods is not only theoretically interesting but is also crucial in comprehending the interaction between the wave and materials in more advanced uses, including energy harvesting, smart materials, and metamaterials. As a longitudinal wave moves in an MEE circular rod, it leads to mechanical stress and strain. This leads to the creation of electric fields and charges in the rod because of the piezoelectric effect. Concurrently, the magnetic field and magnetization change as a result of the magneto-strictive effect. These inter-field effects change the apparent stiffness and mass density of the rod, affect the wave propagation speed, and produce dispersion [27].

To this effect, a non-uniform nonlinear dispersive wave equation incorporating magneto-electric coupling and a transverse Poisson deformation can be developed as [28]:

$$\frac{\partial^2 f}{\partial t^2} - v^2 \frac{\partial^2 f}{\partial x^2} - \frac{\partial^2}{\partial x^2}\left(\frac{v^2}{2} f^2 + Q \frac{\partial^2 f}{\partial t^2}\right) = 0, \tag{1.1}$$

where (x) and (t) are the space and time variables, $f(x,t)$ is the wave function, (v) is the linear wave velocity, which is a function of the elastic modulus of the material and the mass density of the material, and (M) is the coefficient that takes into account the effects of dispersion caused by transverse coupling. The model is a reflection of the behavior of MEE rods operating under a limited number of assumptions, namely the exertion of "axil" symmetry and limitation of the deformation in a radial direction. To simplify the generalization of this model to non-idealized applications and to provide a framework into which the nonlocal and memory-dependent phenomena of magneto-electro-elastic (MEE) media can be integrated, we rewrite Eq (1.1) using the conformable fractional derivative. This fractional extension enables the governing equation to include the hereditary and viscoelastic contributions that are commonly ignored by classical integer-order models. These effects are important in the description of the long-range temporal relations and spatial interactions of complex media. As a result, the corresponding fractional wave model is a more flexible and physically meaningful picture of nonlinear wave propagation. In addition, the analytical study conducted in this paper does not only lead to the discovery of new categories of precise solutions, such as dark kink-like solitons, but also will reveal how the amplitude, stability, and dynamical development of these nonlinear waves depend on the fractional order, which can be viewed as a more profound understanding of the interplay between dispersion, nonlinearity, and fractional dynamics.

$$D_{tt}^{2\alpha} f - v^2 D_{xx}^{2\alpha} f - D_{xx}^{2\alpha}\left(\frac{v^2}{2} f^2 + Q D_{tt}^{2\alpha} f\right) = 0, \quad 0 \le \alpha < 1, \quad t > 0. \tag{1.2}$$

Within this system, the operator (D^α) is the conformable fractional partial derivative of order (α), which follows the definition described in reference [29]. The conformable fractional derivative of Eq (1.1) is used to increase the flexibility and precision of the fractional nonlinear dispersive wave model used to model the complex interactions in the magneto-electro-elastic (MEE) medium. In contrast to the Caputo and Riemann-Liouville derivatives, where the nonlocal integral kernel of the derivative can make treatment of the operator difficult, the conformable derivative is local and maintains the key calculus properties in analysis including the chain and product rules. This permits the transformation of the fractional model to solvable ordinary differential equations by such analytical methods as the generalized Riccati-Bernoulli sub-ODE technique. Additionally, the conformable formulation directly and physically describes the transverse Poisson effect, dispersion, and field coupling in MEE structures, and thus gives a better understanding of soliton dynamics, bifurcation, and mechanisms of energy exchange.

$$G^\alpha(g)(x) = \lim_{\kappa \to 0} \frac{g(x + \kappa x^{1-\alpha}) - g(x)}{\kappa}, \quad 0 < \alpha \leq 1. \tag{1.3}$$

$$\begin{cases} G^\alpha(k_1 U + k_2 V) = k_1 G^\alpha(U) + k_2 G^\alpha(V). \\ G^\alpha(UV)(x) = V(x) G^\alpha(U)(x) + U(x) G^\alpha(V)(x). \\ G^\alpha\left(\dfrac{V}{U}\right)(x) = \dfrac{U(x) G^\alpha(V)(x) - V(x) G^\alpha(U)(x)}{U(x)^2}. \\ G^\alpha(V(U(x))) = V'(U(x)) G^\alpha(U)(x). \end{cases} \tag{1.4}$$

The existence of soliton solutions of nonlinear wave equations has led researchers to develop several analysis techniques to apply to the various solutions of the nonlinear equations due to their critical nature in the development of advanced technologies in various fields like aerospace, meteorology, biotechnology, and communication engineering. Particularly, the nonlinear dynamic model relevant to that discussed in this study has been subjected to much research, such as the studies by Seadawy and Manafian [30], Durur et al. [31], Islam et al. [32], Iqbal et al. [33], Baskonus et al. [34], Sajid and Akram [35], and Xue et al. [36] which investigating the phenomenon of solitons and wave propagation characteristics. Aljahdaly et al. [37] recently used the generalized exponential rational function method (GERFM) with nonlinear longitudinal wave equation in an MEE circular rod and found different exact and stable soliton solutions.

These works have, however, mostly not been brought to bear on the fractional structure of the governing Eq (1.1) or even with the use of the generalized Riccati-Bernoulli sub-ODE method with Bäcklund transformation in the conformable and simple definition of the fractional derivative. To fill in this gap, this paper will examine a fractional analog of the magneto-electro-elastic longitudinal wave equation in the presence of external fields, taking into account zero conductivity and multiple coupled fields. With the introduction of a conformable fractional operator, a more general structure of mathematics is obtained with increased flexibility in modeling memory-dependent and nonlocal dependencies and terms compared to their classical counterparts, but still possesses classical features such as the chain rule. The present work is therefore an orderly examination of a system of how the fractional-order parameter (α) affects qualitative dynamics of the resultant soliton solutions, in particular through careful analyses of stability, bifurcation, and sensitivity. In order to evaluate the response of the model to tiny perturbations, one adopts the linear stability method, whereas the

influence of physical and geometric parameters on the properties of solutions is determined through sensitivity analysis. The results of solving the novel soliton solutions by the proposed method also prove the strength and usefulness of this methodology to trickier fractional nonlinear models. Moreover, the results confirm the prospects of the model enhancing the concept of wave propagation in fractional MEE media and helping improve of superior smart materials-related technologies.

2. Methodology

The work proposes an improved mathematical model to obtain the exact solutions to space-time fractional partial differential equations (FPDEs), which can serve as a potential framework for describing nonlinear wave scattering phenomena in magneto-electro-elastic (MEE) materials. It combines the generalized transform of waves, fractional balancing, and deformed Riccati-Bernoulli sub-ODE approach to produce new soliton solutions. The methodological steps are as follows:

2.1. Reduction of the FPDE to an ODE

The generalized fractional PDE to be considered is as follows:

$$\mathfrak{R}_1\left(f, D^{\alpha_l}(f), D^{\alpha}_{\wp}(f), D^{2\alpha}_{\wp_2}(f), fD^{\alpha}_{\wp_3}(f), \ldots\right) = 0, \quad 0 < \alpha \leq 1, \tag{2.1}$$

where (D^{α}) is the conformable fractional derivative and $f = f(x,t)$ is the wave function. A transformation of this kind under which a wave evolves conformably is brought out:

$$\wp(x,t) = \frac{x^{\alpha}}{\alpha} - \frac{\omega t^{\alpha}}{\alpha}. \tag{2.2}$$

The original FPDE can be transformed by the above transformation, consequently reducing to an ODE of the form:

$$\mathfrak{R}_2\left(F, \frac{dF}{d\wp}, \frac{d^2F}{d\wp^2}, F\frac{d^3F}{d\wp^3}, \ldots\right) = 0. \tag{2.3}$$

2.2. Ansatz construction via generalized rational expansion

The goal of solving the reduced ODE can be achieved by using a rational functional ansatz:

$$f(\wp) = \sum_{i=-w}^{w} a_i \gamma(\wp)^i, \tag{2.4}$$

where the coefficient (a_i) need to be found and $\gamma(\wp)$ is represented by Bäcklund transformation:

$$\gamma(\wp) = \frac{-\beta k_2 + k_1 \aleph(\wp)}{k_1 + k_2 \aleph(\wp)}, \tag{2.5}$$

where $k_1, k_2 \in \mathrm{R}$ with $k_2 \neq 0$. $\aleph(\wp)$ satisfies a generalized Riccati-Bernoulli equation:

$$\frac{d\aleph}{d\wp} = \beta + \aleph(\wp)^2. \tag{2.6}$$

Depending on the sign of (β), different versions of solutions of (β) can appear-trigonometric, hyperbolic, and rational solutions-and it has great flexibility in representing nonlinear wave profiles [38].

Type I solutions ($\beta < 0$): The solutions containing functions such as

$$\begin{aligned}
\aleph_1(\wp) &= -\sqrt{-\beta}\tanh_{rs}(\sqrt{-\beta}\wp),\\
\aleph_2(\wp) &= -\sqrt{-\beta}\coth_{rs}(\sqrt{-\beta}\wp),\\
\aleph_3(\wp) &= -\sqrt{-\beta}\tanh_{rs}(2\sqrt{-\beta}\wp) \pm i\sqrt{-\beta}\,\mathrm{sech}_{rs}(2\sqrt{-\beta}\wp),\\
\aleph_4(\wp) &= -\sqrt{-\beta}\coth_{rs}(2\sqrt{-\beta}\wp) \pm \sqrt{-\beta}\,\mathrm{csch}_{rs}(2\sqrt{-\beta}\wp),\\
\aleph_5(\wp) &= -\frac{1}{2}\left(\sqrt{-\beta}\tanh_{rs}\left(\frac{\sqrt{-\beta}}{2}\wp\right) + \sqrt{-\beta}\coth_{rs}\left(\frac{\sqrt{-\beta}}{2}\wp\right)\right),\\
\aleph_6(\wp) &= \frac{\sqrt{-(L^2+M^2)\beta} - L\sqrt{-\beta}\cosh_{rs}(2\sqrt{-\beta}\wp)}{\beta\sinh_{rs}(2\sqrt{-\beta}\wp) + L},\\
\aleph_7(\wp) &= -\frac{\sqrt{-(L^2-M^2)\beta} - L\sqrt{-\beta}\sinh_{rs}(2\sqrt{-\beta}\wp)}{\beta\cosh_{rs}(2\sqrt{-\beta}\wp) + L}.
\end{aligned} \tag{2.7}$$

Type II solutions ($\beta > 0$): The solutions containing functions such as

$$\begin{aligned}
\aleph_8(\wp) &= \sqrt{\beta}\tan_{rs}(\sqrt{\beta}\wp),\\
\aleph_9(\wp) &= -\sqrt{\beta}\cot_{rs}(\sqrt{\beta}\wp),\\
\aleph_{10}(\wp) &= -\sqrt{\beta}\tan_{rs}(2\sqrt{\beta}\wp) \pm \sqrt{\beta}\sec_{rs}(2\sqrt{\beta}\wp),\\
\aleph_{11}(\wp) &= -\sqrt{\beta}\cot_{rs}(2\sqrt{\beta}\wp) \pm \sqrt{\beta}\csc_{rs}(2\sqrt{\beta}\wp),\\
\aleph_{12}(\wp) &= \frac{1}{2}\left(\sqrt{\beta}\tan_{rs}\left(\frac{\sqrt{\beta}}{2}\wp\right) - \sqrt{\beta}\cot_{rs}\left(\frac{\sqrt{\beta}}{2}\wp\right)\right),\\
\aleph_{13}(\wp) &= \frac{\pm\sqrt{(L^2-M^2)\beta} - M\sqrt{\beta}\cos_{rs}(2\sqrt{\beta}\wp)}{M\sin_{rs}(2\sqrt{\beta}\wp) + L},\\
\aleph_{14}(\wp) &= -\frac{\pm\sqrt{(M^2-L^2)\beta} - M\sqrt{\beta}\sin_{rs}(2\sqrt{\beta}\wp)}{M\cos_{rs}(2\sqrt{\beta}\wp) + L}.
\end{aligned} \tag{2.8}$$

Type III solutions ($\beta = 0$): The solutions containing rational like

$$\aleph_{15}(\wp) = \frac{1}{\wp + h}, \quad h \in R. \tag{2.9}$$

The distorted trigonometric function and the hyperbolic functions are as follows with deformation parameters $r > 0$, $s > 0$ to manipulate the wave shape asymmetry and modulation.

$$\sinh_{rs}(\wp) = \frac{re^{\wp} - se^{-\wp}}{2}, \quad \cosh_{rs}(\wp) = \frac{re^{\wp} + se^{-\wp}}{2}, \quad \tanh_{rs}(\wp) = \frac{re^{\wp} - se^{-\wp}}{re^{\wp} + se^{-\wp}},$$
$$\operatorname{csch}_{rs}(\wp) = \frac{2}{re^{\wp} - se^{-\wp}}, \quad \operatorname{sech}_{rs}(\wp) = \frac{2}{re^{\wp} + se^{-\wp}}, \quad \coth_{rs}(\wp) = \frac{re^{\wp} + se^{-\wp}}{re^{\wp} - se^{-\wp}},$$
$$\sin_{rs}(\wp) = \frac{re^{i\wp} - se^{-i\wp}}{2i}, \quad \cos_{rs}(\wp) = \frac{re^{i\wp} + se^{-i\wp}}{2}, \quad \tan_{rs}(\wp) = -i\,\frac{re^{i\wp} - se^{-i\wp}}{re^{i\wp} + se^{-i\wp}},$$
$$\csc_{rs}(\wp) = \frac{2i}{re^{i\wp} - se^{-i\wp}}, \quad \sec_{rs}(\wp) = \frac{2}{re^{i\wp} + se^{-i\wp}}, \quad \cot_{rs}(\wp) = i\,\frac{re^{i\wp} + se^{-i\wp}}{re^{i\wp} - se^{-i\wp}}.$$

2.3. Determination of series expansion order

To ensure compatibility between the nonlinear terms and the highest-order derivatives in the reduced ODE, a homogeneous balancing principle is applied [39]:

$$D\left[\frac{d^m f}{d\wp^m}\right] = w + m, \quad D\left[f^P \frac{d^m f}{d\wp^m}\right]^q = wP + q(m + w). \tag{2.10}$$

This balancing yields the optimal value of (w) for the ansatz structure, ensuring that the assumed solution form can accurately represent the governing dynamics.

2.4. Algebraic system and exact solution extraction

The proposed ansatz is plugged into the ODE, and comparing like powers of $\gamma(\wp)$ in this series, one gets a system for the parameters (a_i), (ω), and (β). The solution of such a system allows us to discover closed-form expressions for soliton amplitudes and shapes, propagation speeds, as well as fractional-order impact. The original solutions to the fractional model are therefore recovered through a re-substitution in terms of the original variables, resulting in a closed-form solution for the fractional-order system.

3. Execution of the problem

We focus here on the determination of the generalized Riccati-Bernoulli sub-ODE method with Bäcklund transformation to give the exact soliton solutions of the conformable space-time fractional longitudinal wave equation in a magneto-electro-elastic (MEE) rod of a circular shape. To accomplish this, the fractional governing equation is initially transformed into an ordinary differential equation (ODE) through the substitution of a wave transformation, $\wp(x,t) = \frac{x^\alpha}{\alpha} - \frac{\omega t^\alpha}{\alpha}$. This substitution reduces the analysis of the equation to a nonlinear ODE in terms of the traveling wave variable.

$$-v^2\left[(1+F)\frac{d^2F}{d\wp^2}\right] - v^2\left(\frac{dF}{d\wp}\right)^2 + \omega^2\left(\frac{d^2F}{d\wp^2} - Q\frac{d^4F}{d\wp^4}\right) = 0. \tag{3.1}$$

To derive the reduced form, Eq (3.1) is first rearranged as

$$\omega^2 Q\frac{d^4F}{d\wp^4} + v^2(1+F)\frac{d^2F}{d\wp^2} + v^2\left(\frac{dF}{d\wp}\right)^2 - \omega^2\frac{d^2F}{d\wp^2} = 0. \tag{3.2}$$

Integrating once with respect to $\wp$ gives

$$\omega^2 Q\frac{d^3F}{d\wp^3} + v^2(1+F)\frac{dF}{d\wp} - \omega^2\frac{dF}{d\wp} = C_1, \tag{3.3}$$

where the identity $\int(1+F)F''\,d\wp = (1+F)F' - \int(F')^2\,d\wp$ has been used to cancel the terms involving $(F')^2$. Integrating again with respect to $\wp$ yields

$$\omega^2 Q\frac{d^2F}{d\wp^2} + v^2\left(F + \frac{1}{2}F^2\right) - \omega^2 F = C_1\wp + C_2. \tag{3.4}$$

Rearranging, we obtain

$$(\omega^2 - v^2)F - \frac{v^2}{2}F^2 - \omega^2 Q\frac{d^2F}{d\wp^2} = -\left(C_1\wp + C_2\right). \tag{3.5}$$

For bounded vibration modes of the magneto-electro-elastic (MEE) rod, physically relevant boundary conditions eliminate secular or unbounded terms:

- $C_1 = 0$ ensures that no term grows linearly with $\wp$, maintaining bounded displacement and finite energy.
- $C_2 = 0$ corresponds to selecting a zero reference level of displacement, consistent with symmetric or vanishing boundary conditions.

Applying $C_1 = C_2 = 0$ simplifies the expression to the desired second-order nonlinear ODE:

$$(\omega^2 - v^2)F - \frac{v^2}{2}F^2 - \omega^2 Q\frac{d^2F}{d\wp^2} = 0. \tag{3.6}$$

The expressions contain model parameters like wave velocity (v), frequency (ω), and dispersion constant (Q). Matching the powers between the nonlinearity (F^2) and highest-order derivative, we conclude that the degree of the solution is 2. Putting the general form of the solution into the simplified ODE and using the standard algorithm of the proposed method, we obtain a number of distinct exact solutions. The different assumptions on the parameter (β) allow the existence of three broad categories of solutions, which are then discussed and analyzed further concerning their mathematical interpretation. The retrieved solitons are found to exhibit very interesting dynamics that can help shed light on the behavior of the nonlinear propagation of waves in the MEE media when such a propagation is affected by fractional-order effects.

Case 1.

$$a_1 = 0, a_{-1} = 0, a_0 = -3\,\frac{-\omega^2 + v^2}{v^2}, a_{-2} = -\frac{3}{4}\,\frac{\left(-\omega^2 + v^2\right)^2}{\omega^2 Q v^2}, a_2 = 0, \omega = \omega, \beta = \frac{1}{4}\,\frac{-\omega^2 + v^2}{\omega^2 Q}. \tag{3.7}$$

Case 2.

$$\begin{aligned} a_1 = 0, a_{-1} = 0, a_0 = -\frac{3}{2}\,\frac{-\omega^2 + v^2}{v^2}, a_{-2} = -\frac{3}{64}\,\frac{\omega^4 - 2\,v^2\omega^2 + v^4}{\omega^2 Q v^2}, \\ a_2 = -12\,\frac{\omega^2 Q}{v^2}, \omega = \omega, \beta = \frac{1}{16}\,\frac{-\omega^2 + v^2}{\omega^2 Q}. \end{aligned} \tag{3.8}$$

Identifying the above founded solutions sets, we have obtained analytical solution to the hyperbolic soliton modeling the governing conformable fractional model, which may be described by the following analytical form corresponding to Case 1, where ($\beta < 0$) and $\wp = \frac{x^\alpha}{\alpha} - \frac{\omega t^\alpha}{\alpha}$

$$f_1(x,t) = -3/4\,\frac{\left(-\omega^2+v^2\right)^2\left(k_1 - k_2\sqrt{-\beta}\tanh\left(\sqrt{-\beta}\,(\wp)\right)\right)^2}{\omega^2 Q v^2\left(-\beta k_2 - k_1\sqrt{-\beta}\tanh\left(\sqrt{-\beta}\,(\wp)\right)\right)^2} - 3\,\frac{-\omega^2+v^2}{v^2}, \tag{3.9}$$

$$f_2(x,t) = -3/4\,\frac{\left(-\omega^2+v^2\right)^2\left(k_1 - k_2\sqrt{-\beta}\coth\left(\sqrt{-\beta}\,(\wp)\right)\right)^2}{\omega^2 Q v^2\left(-\beta k_2 - k_1\sqrt{-\beta}\coth\left(\sqrt{-\beta}\,(\wp)\right)\right)^2} - 3\,\frac{-\omega^2+v^2}{v^2}, \tag{3.10}$$

$$\begin{aligned} f_3(x,t) = &-3/4\,\frac{\left(-\omega^2+v^2\right)^2\left(k_1 + k_2\left(-\sqrt{-\beta}\tanh\left(2\sqrt{-\beta}\,(\wp)\right) \pm \left(i\sqrt{-\beta}sech\left(2\sqrt{-\beta}\,(\wp)\right)\right)\right)\right)^2}{\omega^2 Q v^2\left(-\beta k_2 + k_1\left(-\sqrt{-\beta}\tanh\left(2\sqrt{-\beta}\,(\wp)\right) \pm \left(i\sqrt{-\beta}sech\left(2\sqrt{-\beta}\,(\wp)\right)\right)\right)\right)^2} \\ &- 3\,\frac{-\omega^2+v^2}{v^2}, \end{aligned} \tag{3.11}$$

$$\begin{aligned} f_4(x,t) = &-3/4\,\frac{\left(-\omega^2+v^2\right)^2\left(k_1 + k_2\left(-\sqrt{-\beta}\coth\left(2\sqrt{-\beta}\,(\wp)\right) \pm \left(\sqrt{-\beta}csch\left(2\sqrt{-\beta}\,(\wp)\right)\right)\right)\right)^2}{\omega^2 Q v^2\left(-\beta k_2 + k_1\left(-\sqrt{-\beta}\coth\left(2\sqrt{-\beta}\,(\wp)\right) \pm \left(\sqrt{-\beta}csch\left(2\sqrt{-\beta}\,(\wp)\right)\right)\right)\right)^2} \\ &- 3\,\frac{-\omega^2+v^2}{v^2}, \end{aligned} \tag{3.12}$$

$$\begin{aligned} f_5(x,t) = &-3/4\,\frac{\left(-\omega^2+v^2\right)^2\left(k_1 + k_2\left(-1/2\sqrt{-\beta}\tanh\left(1/2\sqrt{-\beta}\,(\wp)\right) - 1/2\sqrt{-\beta}\coth\left(1/2\sqrt{-\beta}\,(\wp)\right)\right)\right)^2}{\omega^2 Q v^2\left(-\beta k_2 + k_1\left(-1/2\sqrt{-\beta}\tanh\left(1/2\sqrt{-\beta}\,(\wp)\right) - 1/2\sqrt{-\beta}\coth\left(1/2\sqrt{-\beta}\,(\wp)\right)\right)\right)^2} \\ &- 3\,\frac{-\omega^2+v^2}{v^2}, \end{aligned} \tag{3.13}$$

$$f_6(x,t) = -3/4\,\frac{\left(-\omega^2+v^2\right)^2\left(k_1 + \frac{k_2\left(\sqrt{-\left(L^2+M^2\right)\beta} - L\sqrt{-\beta}\cosh\left(2\sqrt{-\beta}(\wp)\right)\right)}{L\sinh\left(2\sqrt{-\beta}(\wp)\right)+M}\right)^2}{\omega^2 Q^1 v^2\left(-\beta k_2 + \frac{k_1\left(\sqrt{-\left(L^2+M^2\right)\beta} - L\sqrt{-\beta}\cosh\left(2\sqrt{-\beta}(\wp)\right)\right)}{L\sinh\left(2\sqrt{-\beta}(\wp)\right)+M}\right)^2} - 3\,\frac{-\omega^2+v^2}{v^2}, \tag{3.14}$$

$$f_7(x,t) = -3/4\,\frac{\left(-\omega^2+v^2\right)^2\left(k_1 + \frac{k_2\left(\sqrt{-\left(L^2-M^2\right)\beta} - L\sqrt{-\beta}\sinh\left(2\sqrt{-\beta}(\wp)\right)\right)}{L\cosh\left(2\sqrt{-\beta}(\wp)\right)+M}\right)^2}{\omega^2 Q^1 v^2\left(-\beta k_2 + \frac{k_1\left(\sqrt{-\left(L^2-M^2\right)\beta} - L\sqrt{-\beta}\sinh\left(2\sqrt{-\beta}(\wp)\right)\right)}{L\cosh\left(2\sqrt{-\beta}(\wp)\right)+M}\right)^2} - 3\,\frac{-\omega^2+v^2}{v^2}. \tag{3.15}$$

Here, we have obtained analytical solutions to the trigonometric soliton modeling the governing conformable fractional model, which may be described by the following analytical form corresponding to Case 1, where ($\beta > 0$) and $\wp = \frac{x^\alpha}{\alpha} - \frac{\omega t^\alpha}{\alpha}$

$$f_8(x,t) = -3/4\,\frac{\left(-\omega^2+v^2\right)^2\left(k_1+k_2\sqrt{\beta}\tan\left(\sqrt{\beta}\,(\wp)\right)\right)^2}{\omega^2 Q v^2\left(-\beta\,k_2+k_1\sqrt{\beta}\tan\left(\sqrt{\beta}\,(\wp)\right)\right)^2} - 3\,\frac{-\omega^2+v^2}{v^2}, \tag{3.16}$$

$$f_9(x,t) = -3/4\,\frac{\left(-\omega^2+v^2\right)^2\left(k_1-k_2\sqrt{\beta}\cot\left(\sqrt{\beta}\,(\wp)\right)\right)^2}{\omega^2 Q v^2\left(-\beta\,k_2-k_1\sqrt{\beta}\cot\left(\sqrt{\beta}\,(\wp)\right)\right)^2} - 3\,\frac{-\omega^2+v^2}{v^2}, \tag{3.17}$$

$$f_{10}(x,t) = -\frac{3}{4}\,\frac{(-\omega^2+v^2)^2\left(k_1+k_2(-\sqrt{\beta}\tan(2\sqrt{\beta}\wp)\pm\sqrt{\beta}\sec(2\sqrt{\beta}\wp))\right)^2}{\omega^2 Q v^2\left(-\beta k_2+k_1(-\sqrt{\beta}\tan(2\sqrt{\beta}\wp)\pm\sqrt{\beta}\sec(2\sqrt{\beta}\wp))\right)^2} + 3\,\frac{\omega^2-v^2}{v^2}.$$

$$f_{11}(x,t) = -3/4\,\frac{\left(-\omega^2+v^2\right)^2\left(k_1+k_2\left(-\sqrt{\beta}\cot\left(2\sqrt{\beta}\,(\pm)\right)\pm\left(\sqrt{\beta}\csc\left(2\sqrt{\beta}\,(\wp)\right)\right)\right)\right)^2}{\omega^2 Q v^2\left(-\beta\,k_2+k_1\left(-\sqrt{\beta}\cot\left(2\sqrt{\beta}\,(\wp)\right)\pm\left(\sqrt{\beta}\csc\left(2\sqrt{\beta}\,(\wp)\right)\right)\right)\right)^2} - 3\,\frac{-\omega^2+v^2}{v^2}, \tag{3.18}$$

$$f_{12}(x,t) = -3/4\,\frac{\left(-\omega^2+v^2\right)^2\left(k_1+k_2\left(1/2\sqrt{\beta}\tan\left(1/2\sqrt{\beta}\,(\wp)\right)-1/2\sqrt{\beta}\cot\left(1/2\sqrt{\beta}\,(\wp)\right)\right)\right)^2}{\omega^2 Q v^2\left(-\beta\,k_2+k_1\left(1/2\sqrt{\beta}\tan\left(1/2\sqrt{\beta}\,(\wp)\right)-1/2\sqrt{\beta}\cot\left(1/2\sqrt{\beta}\,(\wp)\right)\right)\right)^2} - 3\,\frac{-\omega^2+v^2}{v^2}, \tag{3.19}$$

$$f_{13}(x,t) = -3/4\,\frac{\left(-\omega^2+v^2\right)^2\left(k_1+\frac{k_2\left(\pm\left(\sqrt{(L^2-M^2)\delta}\right)-L\sqrt{\beta}\cos\left(2\sqrt{\beta}(\wp)\right)\right)}{L\sin\left(2\sqrt{\beta}(\wp)\right)+M}\right)^2\omega^{-2}}{Q^1 v^2\left(-\beta\,k_2+\frac{k_1\left(\pm\left(\sqrt{(L^2-M^2)\delta}\right)-L\sqrt{\beta}\cos\left(2\sqrt{\beta}(\wp)\right)\right)}{L\sin\left(2\sqrt{\beta}(\wp)\right)+M}\right)^2} - 3\,\frac{-\omega^2+v^2}{v^2}, \tag{3.20}$$

$$f_{14}(x,t) = -3/4\,\frac{\left(-\omega^2+v^2\right)^2\left(k_1+\frac{k_2\left(\pm\left(\sqrt{(L^2-M^2)\beta}\right)-L\sqrt{\beta}\sin\left(2\sqrt{\beta}(\wp)\right)\right)}{L\cos\left(2\sqrt{\beta}(\wp)\right)+M}\right)^2}{\omega^2 Q^1 v^2\left(-\beta\,k_2+\frac{k_1\left(\pm\left(\sqrt{(L^2-M^2)\beta}\right)-L\sqrt{\beta}\sin\left(2\sqrt{\beta}(\wp)\right)\right)}{L\cos\left(2\sqrt{\beta}(\wp)\right)+M}\right)^2} - 3\,\frac{-\omega^2+v^2}{v^2}. \tag{3.21}$$

Here, we have obtained analytical solutions to the rational soliton modeling the governing conformable fractional model, which may be described by the following analytical form corresponding to Case 1, where ($\beta = 0$) and $\wp = \frac{x^\alpha}{\alpha} - \frac{\omega t^\alpha}{\alpha}$

$$f_{15}(x,t) = -3/4\,\frac{\left(-\omega^2+v^2\right)^2\left(k_1-\frac{k_2}{\wp+w}\right)^2}{\omega^2 Q v^2\left(-1/4\,\frac{\left(-\omega^2+v^2\right)k_2}{\omega^2 Q}-\frac{k_1}{\wp+w}\right)^2} - 3\,\frac{-\omega^2+v^2}{v^2}. \tag{3.22}$$

Identifying the above founded solutions sets, we have obtained analytical solution to the hyperbolic soliton modeling the governing conformable fractional model, which may be described by the following analytical form corresponding to Case 2, where ($\beta < 0$) and $\wp = \frac{x^\alpha}{\alpha} - \frac{\omega t^\alpha}{\alpha}$

$$f_{16}(x,t) = -\frac{3}{64}\frac{\left(\omega^4 - 2\,v^2\omega^2 + v^4\right)\left(k_1 - k_2\sqrt{-\beta}\tanh\left(\sqrt{-\beta}\,(\wp)\right)\right)^2}{\omega^2 Q v^2\left(-\beta\,k_2 - k_1\sqrt{-\beta}\tanh\left(\sqrt{-\beta}\,(\wp)\right)\right)^2} - 3/2\,\frac{-\omega^2 + v^2}{v^2} - 12\,\frac{\omega^2 Q\left(-\beta\,k_2 - k_1\sqrt{-\beta}\tanh\left(\sqrt{-\beta}\,(\wp)\right)\right)^2}{v^2\left(k_1 - k_2\sqrt{-\beta}\tanh\left(\sqrt{-\beta}\,(\wp)\right)\right)^2}, \tag{3.23}$$

$$f_{17}(x,t) = -\frac{3}{64}\frac{\left(\omega^4 - 2\,v^2\omega^2 + v^4\right)\left(k_1 - k_2\sqrt{-\beta}\coth\left(\sqrt{-\beta}\,(\wp)\right)\right)^2}{\omega^2 Q v^2\left(-\beta\,k_2 - k_1\sqrt{-\beta}\coth\left(\sqrt{-\beta}\,(\wp)\right)\right)^2} - 3/2\,\frac{-\omega^2 + v^2}{v^2} - 12\,\frac{\omega^2 Q\left(-\beta\,k_2 - k_1\sqrt{-\beta}\coth\left(\sqrt{-\beta}\,(\wp)\right)\right)^2}{v^2\left(k_1 - k_2\sqrt{-\beta}\coth\left(\sqrt{-\beta}\,(\wp)\right)\right)^2}, \tag{3.24}$$

$$f_{18}(x,t) = -\frac{3}{64}\frac{\left(\omega^4 - 2\,v^2\omega^2 + v^4\right)\left(k_1 + k_2\left(-\sqrt{-\beta}\tanh\left(2\,\sqrt{-\beta}\,(\wp)\right) \pm \left(i\,\sqrt{-\beta}sech\left(2\,\sqrt{-\beta}\,(\wp)\right)\right)\right)\right)^2}{\omega^2 Q v^2\left(-\beta\,k_2 + k_1\left(-\sqrt{-\beta}\tanh\left(2\,\sqrt{-\beta}\,(\wp)\right) \pm \left(i\,\sqrt{-\beta}sech\left(2\,\sqrt{-\beta}\,(\wp)\right)\right)\right)\right)^2} - 3/2\,\frac{-\omega^2 + v^2}{v^2} - 12\,\frac{\omega^2 Q\left(-\beta\,k_2 + k_1\left(-\sqrt{-\beta}\tanh\left(2\,\sqrt{-\beta}\,(\wp)\right) \pm \left(i\,\sqrt{-\beta}sech\left(2\,\sqrt{-\beta}\,(\wp)\right)\right)\right)\right)^2}{v^2\left(k_1 + k_2\left(-\sqrt{-\beta}\tanh\left(2\,\sqrt{-\beta}\,(\wp)\right) \pm \left(i\,\sqrt{-\beta}sech\left(2\,\sqrt{-\beta}\,(\wp)\right)\right)\right)\right)^2}, \tag{3.25}$$

$$f_{19}(x,t) = -\frac{3}{64}\frac{\left(\omega^4 - 2\,v^2\omega^2 + v^4\right)\left(k_1 + k_2\left(-\sqrt{-\beta}\coth\left(2\,\sqrt{-\beta}\,(\wp)\right) \pm \left(\sqrt{-\beta}csch\left(2\,\sqrt{-\beta}\,(\wp)\right)\right)\right)\right)^2}{\omega^2 Q v^2\left(-\beta\,k_2 + k_1\left(-\sqrt{-\beta}\coth\left(2\,\sqrt{-\beta}\,(\wp)\right) \pm \left(\sqrt{-\beta}csch\left(2\,\sqrt{-\beta}\,(\wp)\right)\right)\right)\right)^2} - 3/2\,\frac{-\omega^2 + v^2}{v^2} - 12\,\frac{\omega^2 Q\left(-\beta\,k_2 + k_1\left(-\sqrt{-\beta}\coth\left(2\,\sqrt{-\beta}\,(\wp)\right) \pm \left(\sqrt{-\beta}csch\left(2\,\sqrt{-\beta}\,(\wp)\right)\right)\right)\right)^2}{v^2\left(k_1 + k_2\left(-\sqrt{-\beta}\coth\left(2\,\sqrt{-\beta}\,(\wp)\right) \pm \left(\sqrt{-\beta}csch\left(2\,\sqrt{-\beta}\,(\wp)\right)\right)\right)\right)^2}, \tag{3.26}$$

$$
\begin{aligned}
f_{20}(x,t) = &-\frac{3}{64}\frac{\left(\omega^4-2\,v^2\omega^2+v^4\right)\left(k_1+k_2\left(-1/2\,\sqrt{-\beta}\tanh\left(1/2\,\sqrt{-\beta}\,(\wp)\right)-1/2\,\sqrt{-\beta}\coth\left(1/2\,\sqrt{-\beta}\,(\wp)\right)\right)\right)^2}{\omega^2 Q v^2\left(-\beta\,k_2+k_1\left(-1/2\,\sqrt{-\beta}\tanh\left(1/2\,\sqrt{-\beta}\,(\wp)\right)-1/2\,\sqrt{-\beta}\coth\left(1/2\,\sqrt{-\beta}\,(\wp)\right)\right)\right)^2}\\
&-\frac{3}{2}\frac{-\omega^2+v^2}{v^2}\\
&-12\,\frac{\omega^2 Q\left(-\beta\,k_2+k_1\left(-1/2\,\sqrt{-\beta}\tanh\left(1/2\,\sqrt{-\beta}\,(\wp)\right)-1/2\,\sqrt{-\beta}\coth\left(1/2\,\sqrt{-\beta}\,(\wp)\right)\right)\right)^2}{v^2\left(k_1+k_2\left(-1/2\,\sqrt{-\beta}\tanh\left(1/2\,\sqrt{-\beta}\,(\wp)\right)-1/2\,\sqrt{-\beta}\coth\left(1/2\,\sqrt{-\beta}\,(\wp)\right)\right)\right)^2},
\end{aligned}
\tag{3.27}
$$

$$
\begin{aligned}
f_{21}(x,t) = &-\frac{3}{64}\frac{\left(\omega^4-2\,v^2\omega^2+v^4\right)\left(k_1+\frac{k_2\left(\sqrt{-\left(L^2+M^2\right)\beta}-L\sqrt{-\beta}\cosh\left(2\sqrt{-\beta}(\wp)\right)\right)}{L\sinh\left(2\sqrt{-\beta}(\wp)\right)+M}\right)^2}{\omega^2 Q v^2\left(-\beta\,k_2+\frac{k_1\left(\sqrt{-\left(L^2+M^2\right)\beta}-L\sqrt{-\beta}\cosh\left(2\sqrt{-\beta}(\wp)\right)\right)}{L\sinh\left(2\sqrt{-\beta}(\wp)\right)+M}\right)^2}-3/2\,\frac{-\omega^2+v^2}{v^2}\\
&-\frac{12\,\omega^2 Q\left(-\beta\,k_2+\frac{k_1\left(\sqrt{-\left(L^2+M^2\right)\beta}-L\sqrt{-\beta}\cosh\left(2\sqrt{-\beta}(\wp)\right)\right)}{L\sinh\left(2\sqrt{-\beta}(\wp)\right)+M}\right)^2}{v^2\left(k_1+\frac{k_2\left(\sqrt{-\left(L^2+M^2\right)\beta}-L\sqrt{-\beta}\cosh\left(2\sqrt{-\beta}(\wp)\right)\right)}{L\sinh\left(2\sqrt{-\beta}(\wp)\right)+M}\right)^2},
\end{aligned}
\tag{3.28}
$$

$$
\begin{aligned}
f_{22}(x,t) = &-\frac{3}{64}\frac{\left(\omega^4-2\,v^2\omega^2+v^4\right)\left(k_1+\frac{k_2\left(\sqrt{-\left(L^2-M^2\right)\beta}-L\sqrt{-\beta}\sinh\left(2\sqrt{-\beta}(\wp)\right)\right)}{L\cosh\left(2\sqrt{-\beta}(\wp)\right)+M}\right)^2}{\omega^2 Q v^2\left(-\beta\,k_2+\frac{k_1\left(\sqrt{-\left(L^2-M^2\right)\beta}-L\sqrt{-\beta}\sinh\left(2\sqrt{-\beta}(\wp)\right)\right)}{L\cosh\left(2\sqrt{-\beta}(\wp)\right)+M}\right)^2}-3/2\,\frac{-\omega^2+v^2}{v^2}\\
&-\frac{12\,\omega^2 Q\left(-\beta\,k_2+\frac{k_1\left(\sqrt{-\left(L^2-M^2\right)\beta}-L\sqrt{-\beta}\sinh\left(2\sqrt{-\beta}(\wp)\right)\right)}{L\cosh\left(2\sqrt{-\beta}(\wp)\right)+M}\right)^2}{v^2\left(k_1+\frac{k_2\left(\sqrt{-\left(L^2-M^2\right)\beta}-L\sqrt{-\beta}\sinh\left(2\sqrt{-\beta}(\wp)\right)\right)}{L\cosh\left(2\sqrt{-\beta}(\wp)\right)+M}\right)^2}.
\end{aligned}
\tag{3.29}
$$

Here, we have obtained analytical solution to trigonometric soliton modeling the governing conformable fractional model, which may be described by the following analytical form corresponding to Case 2, where ($\beta > 0$) and $\wp = \frac{x^\alpha}{\alpha} - \frac{\omega\, t^\alpha}{\alpha}$

$$
\begin{aligned}
f_{23}(x,t) = &-\frac{3}{64}\frac{\left(\omega^4-2\,v^2\omega^2+v^4\right)\left(k_1+k_2\sqrt{\beta}\tan\left(\sqrt{\beta}\,(\wp)\right)\right)^2}{\omega^2 Q v^2\left(-\beta\,k_2+k_1\sqrt{\beta}\tan\left(\sqrt{\beta}\,(\wp)\right)\right)^2}-3/2\,\frac{-\omega^2+v^2}{v^2}\\
&-12\,\frac{\omega^2 Q\left(-\beta\,k_2+k_1\sqrt{\beta}\tan\left(\sqrt{\beta}\,(\wp)\right)\right)^2}{v^2\left(k_1+k_2\sqrt{\beta}\tan\left(\sqrt{\beta}\,(\wp)\right)\right)^2},
\end{aligned}
\tag{3.30}
$$

$$f_{24}(x,t) = -\frac{3}{64}\frac{\left(\omega^4 - 2\,v^2\omega^2 + v^4\right)\left(k_1 - k_2\,\sqrt{\beta}\cot\left(\sqrt{\beta}\,(\wp)\right)\right)^2}{\omega^2 Q v^2\left(-\beta\,k_2 - k_1\,\sqrt{\beta}\cot\left(\sqrt{\beta}\,(\wp)\right)\right)^2} - 3/2\,\frac{-\omega^2 + v^2}{v^2} - 12\,\frac{\omega^2 Q\left(-\beta\,k_2 - k_1\,\sqrt{\beta}\cot\left(\sqrt{\beta}\,(\wp)\right)\right)^2}{v^2\left(k_1 - k_2\,\sqrt{\beta}\cot\left(\sqrt{\beta}\,(\wp)\right)\right)^2}, \tag{3.31}$$

$$f_{25}(x,t) = -\frac{3}{64}\frac{\left(\omega^4 - 2\,v^2\omega^2 + v^4\right)\left(k_1 + k_2\left(-\sqrt{\beta}\tan\left(2\,\sqrt{\beta}\,(\wp)\right) \pm \left(\sqrt{\beta}\sec\left(2\,\sqrt{\beta}\,(\wp)\right)\right)\right)\right)^2}{\omega^2 Q v^2\left(-\beta\,k_2 + k_1\left(-\sqrt{\beta}\tan\left(2\,\sqrt{\beta}\,(\wp)\right) \pm \left(\sqrt{\beta}\sec\left(2\,\sqrt{\beta}\,(\wp)\right)\right)\right)\right)^2} - 3/2\,\frac{-\omega^2 + v^2}{v^2} - 12\,\frac{\omega^2 Q\left(-\beta\,k_2 + k_1\left(-\sqrt{\beta}\tan\left(2\,\sqrt{\beta}\,(\wp)\right) \pm \left(\sqrt{\beta}\sec\left(2\,\sqrt{\beta}\,(\wp)\right)\right)\right)\right)^2}{v^2\left(k_1 + k_2\left(-\sqrt{\beta}\tan\left(2\,\sqrt{\beta}\,(\wp)\right) \pm \left(\sqrt{\beta}\sec\left(2\,\sqrt{\beta}\,(\wp)\right)\right)\right)\right)^2}, \tag{3.32}$$

$$f_{26}(x,t) = -\frac{3}{64}\frac{\left(\omega^4 - 2\,v^2\omega^2 + v^4\right)\left(k_1 + k_2\left(-\sqrt{\beta}\cot\left(2\,\sqrt{\beta}\,(\wp)\right) \pm \left(\sqrt{\beta}\csc\left(2\,\sqrt{\beta}\,(\wp)\right)\right)\right)\right)^2}{\omega^2 Q v^2\left(-\beta\,k_2 + k_1\left(-\sqrt{\beta}\cot\left(2\,\sqrt{\beta}\,(\wp)\right) \pm \left(\sqrt{\beta}\csc\left(2\,\sqrt{\beta}\,(\wp)\right)\right)\right)\right)^2} - 3/2\,\frac{-\omega^2 + v^2}{v^2} - 12\,\frac{\omega^2 Q\left(-\beta\,k_2 + k_1\left(-\sqrt{\beta}\cot\left(2\,\sqrt{\beta}\,(\wp)\right) \pm \left(\sqrt{\beta}\csc\left(2\,\sqrt{\beta}\,(\wp)\right)\right)\right)\right)^2}{v^2\left(k_1 + k_2\left(-\sqrt{\beta}\cot\left(2\,\sqrt{\beta}\,(\wp)\right) \pm \left(\sqrt{\beta}\csc\left(2\,\sqrt{\beta}\,(\wp)\right)\right)\right)\right)^2}, \tag{3.33}$$

$$f_{27}(x,t) = -\frac{3}{64}\frac{\left(\omega^4 - 2\,v^2\omega^2 + v^4\right)\left(k_1 + k_2\left(1/2\,\sqrt{\beta}\tan\left(1/2\,\sqrt{\beta}\,(\wp)\right) - 1/2\,\sqrt{\beta}\cot\left(1/2\,\sqrt{\beta}\,(\wp)\right)\right)\right)^2}{\omega^2 Q v^2\left(-\beta\,k_2 + k_1\left(1/2\,\sqrt{\beta}\tan\left(1/2\,\sqrt{\beta}\,(\wp)\right) - 1/2\,\sqrt{\beta}\cot\left(1/2\,\sqrt{\beta}\,(\wp)\right)\right)\right)^2} - 3/2\,\frac{-\omega^2 + v^2}{v^2} - 12\,\frac{\omega^2 Q\left(-\beta\,k_2 + k_1\left(1/2\,\sqrt{\beta}\tan\left(1/2\,\sqrt{\beta}\,(\wp)\right) - 1/2\,\sqrt{\beta}\cot\left(1/2\,\sqrt{\beta}\,(\wp)\right)\right)\right)^2}{v^2\left(k_1 + k_2\left(1/2\,\sqrt{\beta}\tan\left(1/2\,\sqrt{\beta}\,(\wp)\right) - 1/2\,\sqrt{\beta}\cot\left(1/2\,\sqrt{\beta}\,(\wp)\right)\right)\right)^2}, \tag{3.34}$$

$$f_{28}(x,t) = -\frac{3}{64}\frac{\left(\omega^4 - 2\,v^2\omega^2 + v^4\right)\left(k_1 + \frac{k_2\left(\pm\left(\sqrt{(L^2-M^2)\beta}\right) - L\,\sqrt{\beta}\cos\left(2\,\sqrt{\beta}(\wp)\right)\right)}{L\sin\left(2\,\sqrt{\beta}(\wp)\right)+M}\right)^2}{\omega^2 Q v^2\left(-\beta\,k_2 + \frac{k_1\left(\pm\left(\sqrt{(L^2-M^2)\delta}\right) - L\,\sqrt{\beta}\cos\left(2\,\sqrt{\beta}(\wp)\right)\right)}{L\sin\left(2\,\sqrt{\beta}(\wp)\right)+M}\right)^2} - 3/2\,\frac{-\omega^2 + v^2}{v^2} - \frac{12\,\omega^2 Q\left(-\beta\,k_2 + \frac{k_1\left(\pm\left(\sqrt{(L^2-M^2)\delta}\right) - L\,\sqrt{\beta}\cos\left(2\,\sqrt{\beta}(\wp)\right)\right)}{L\sin\left(2\,\sqrt{\beta}(\wp)\right)+M}\right)^2}{v^2\left(k_1 + \frac{k_2\left(\pm\left(\sqrt{(L^2-M^2)\delta}\right) - L\,\sqrt{\beta}\cos\left(2\,\sqrt{\beta}(\wp)\right)\right)}{L\sin\left(2\,\sqrt{\beta}(\wp)\right)+M}\right)^2}, \tag{3.35}$$

$$f_{29}(x,t) = -\frac{3}{64}\frac{\left(\omega^4 - 2\,v^2\omega^2 + v^4\right)\left(k_1 + \frac{k_2\left(\pm\left(\sqrt{(L^2-M^2)\beta}\right) - L\sqrt{\beta}\sin\left(2\sqrt{\beta}(\wp)\right)\right)}{L\cos\left(2\sqrt{\beta}(\wp)\right)+M}\right)^2}{\omega^2 Q v^2\left(-\beta\,k_2 + \frac{k_1\left(\pm\left(\sqrt{(L^2-M^2)\beta}\right) - L\sqrt{\beta}\sin\left(2\sqrt{\beta}(\wp)\right)\right)}{L\cos\left(2\sqrt{\beta}(\wp)\right)+M}\right)^2} - 3/2\,\frac{-\omega^2+v^2}{v^2}$$
$$-\frac{12\,\omega^2 Q\left(-\beta\,k_2 + \frac{k_1\left(\pm\left(\sqrt{(L^2-M^2)\beta}\right) - L\sqrt{\beta}\sin\left(2\sqrt{\beta}(\wp)\right)\right)}{L\cos\left(2\sqrt{\beta}(\wp)\right)+M}\right)^2}{v^{-2}\left(k_1 + \frac{k_2\left(\pm\left(\sqrt{(L^2-M^2)\beta}\right) - L\sqrt{\beta}\sin\left(2\sqrt{\beta}(\wp)\right)\right)}{L\cos\left(2\sqrt{\beta}(\wp)\right)+M}\right)^2}. \tag{3.36}$$

Here, I have obtained analytical solution to the trigonometric soliton modeling the governing conformable fractional model, which may be described by the following analytical form corresponding Case 2, where ($\beta = 0$) and $\wp = \frac{x^\alpha}{\alpha} - \frac{\omega t^\alpha}{\alpha}$

$$f_{30}(x,t) = \frac{-\frac{3}{64}\left(\omega^4 - 2\,v^2\omega^2 + v^4\right)\left(k_1 - \frac{k_2}{\wp+w}\right)^2}{\omega^2 Q v^2\left(-1/16\,\frac{\left(-\omega^2+v^2\right)k_2}{\omega^2 Q} - \frac{k_1}{\wp+w}\right)^2} - 3/2\,\frac{-\omega^2+v^2}{v^2} - \frac{12\,\omega^2 Q\left(-1/16\,\frac{\left(-\omega^2+v^2\right)k_2}{\omega^2 Q} - \frac{k_1}{\wp+w}\right)^2}{v^2\left(k_1 - \frac{k_2}{\wp+w}\right)^2}. \tag{3.37}$$

Comparative analysis between the current generalized Riccati-Bernoulli sub-ODE method and generalized exponential rational function method (GERFM) [37] is summarized in Table 1. The GERFM when applied to the nonlinear longitudinal wave equation of a magneto-electro-elastic (MEE) circular rod has been demonstrated to be useful in the creation of an extensive repertoire of analytical wave structures including periodic and solitary. Nevertheless, it covers mainly integer-order models and is based on the exponential trial functions of rationality. However, the present method, which uses the Riccati-Bernoulli sub-ODE and Bäcklund transformation framework, can be extended to fractional-order conformable systems with the ability to derive new dark kink and periodic soliton solutions under identical parameter regimes ($\beta < 0, \quad \beta > 0, \quad$ and $\quad \beta = 0$). Furthermore, the current expression also provides more flexibility to the study of stability, bifurcation structures, and effects of a fractional-order, thus providing more physical insight into the nature of nonlinear spatiotemporal dynamics than the integer models based on the GERFM.

Table 1. A comparative analysis of the current approach and the alternative approach, specifically the generalized exponential rational function method [37].

Case	Generalized Riccati-Bernoulli sub-ODE method	Generalized exponential rational function method
Case I: $\beta < 0$	$f_1 = -3/4\,\frac{\left(-\omega^2+v^2\right)^2(k_1-k_2\sqrt{-\beta}\tanh(\sqrt{-\beta}(\wp)))^2}{\omega^2 Q v^2(-\beta\,k_2-k_1\sqrt{-\beta}\tanh(\sqrt{-\beta}(\wp)))^2} - 3\,\frac{-\omega^2+v^2}{v^2}$,	$\Phi_1(x,t) = C_0\,\mathrm{Sech}^2[-(Fx-vt)]$.
Case II: $\beta > 0$	$f_9 = -3/4\,\frac{\left(-\omega^2+v^2\right)^2(k_1-k_2\sqrt{\beta}\cot(\sqrt{\beta}(\wp)))^2}{\omega^2 Q v^2(-\beta\,k_2-k_1\sqrt{\beta}\cot(\sqrt{\beta}(\wp)))^2} - 3\,\frac{-\omega^2+v^2}{v^2}$,	$\Phi_9(x,t) = -\frac{C_0}{(-\sinh(Fx-tv)-2\cosh(Fx-tv))^2}$.
Case III: $\beta = 0$	$f_{15} = -3/4\,\frac{\left(-\omega^2+v^2\right)^2\left(k_1-\frac{k_2}{\wp+w}\right)^2}{\omega^2 Q v^2\left(-1/4\,\frac{\left(-\omega^2+v^2\right)k_2}{\omega^2 Q} - \frac{k_1}{\wp+w}\right)^2} - 3\,\frac{-\omega^2+v^2}{v^2}$,	$\Phi_{15}(x,t) = -\frac{C_0(5\sin(2(Fx-tv))+6\cos(2(Fx-tv))-8)}{2(\sin(-(Fx-tv))+\cos(-(Fx-tv)))^2}$.

4. Hamiltonian analysis of the system

Here, we move on to carrying out the Hamiltonian analysis on our system by giving an equivalent planar dynamical system to our second-order nonlinear ODE:

$$(\omega^2 - v^2)F - \frac{v^2}{2}F^2 - \omega^2 Q^2 \frac{d^2F}{d\wp^2} = 0. \tag{4.1}$$

Rearranging this to more standard Newtonian form, we get the second derivative term on its own:

$$\frac{d^2F}{d\wp^2} = \frac{1}{\omega^2 Q^2}\left[(\omega^2 - v^2)F - \frac{v^2}{2}F^2\right]. \tag{4.2}$$

Let us define, $y = F(\wp)$ and $g = \frac{dy}{d\wp}$, which transform Eq (4.1) into the following planer dynamical system:

$$\frac{dy}{d\wp} = g, \ \frac{dg}{d\wp} = \frac{1}{\omega^2 Q^2}\left[(\omega^2 - v^2)y - \frac{v^2}{2}y^2\right]. \tag{4.3}$$

The system has the following Hamiltonian with equilibrium points and a jacobian matrix:

$$\begin{aligned} H(y,g) &= \frac{1}{2}g^2 - \frac{1}{\omega^2 Q^2}\left(\frac{1}{2}(\omega^2 - v^2)y^2 - \frac{v^2}{6}y^3\right), \\ (y,g) &= (0,0), \quad \left(\frac{2(\omega^2 - v^2)}{v^2}, 0\right), \end{aligned} \tag{4.4}$$

$$J(y,g) = \begin{pmatrix} 0 & 1 \\ \frac{1}{\omega^2 Q^2}\left(\omega^2 - v^2 - v^2 y\right) & 0 \end{pmatrix}. \tag{4.5}$$

Depending on the eigenvalues of the Jacobian, the nature of any equilibrium point lies in the fact that on any center, the eigenvalue is imaginary, and on any saddle, the eigenvalue is real.

5. Chaotic analysis via perturbation

In order to further analyze our nonlinear system qualitatively we will now look at the possibility of chaos by adding a small external disturbance. Beginning with the planar dynamical system obtained in the Hamiltonian scheme we add a periodic driving force, so that we can trace the reaction of the conservative component toward the outside. The impulsed system has the general form:

$$\begin{aligned} \frac{dy}{d\wp} &= g, \\ \frac{dg}{d\wp} &= \frac{1}{\omega^2 Q^2}\left[(\omega^2 - v^2)y - \frac{v^2}{2}y^2\right] + r_0 cos(v\wp), \end{aligned} \tag{5.1}$$

where (r) and (v) are the amplitude and frequency of external periodic disturbance, respectively. The presence of the forcing term disrupts the Hamiltonian system of the original system of conservation and creates the chance of chaotic dynamics. This is possible because the system has nonlinear structure and it responds easily to external influence. The analytical framework would indicate the

possibility of bifurcation behaviors, sensitive dependence on initial conditions, and evolution of orbit dynamics through the parameters of the system (ν). Such perturbative analysis provides the basis of subsequent utilization of techniques like Melnikov theory, Lyapunov theory, or Poincare surfaces to prove mathematically when the system switches into the chaotic regime.

6. Lyapunov exponent analysis

To further confirm the chaotic nature of the fractional MEE system of Hamilton equations, the largest Lyapunov exponent was determined numerically using the equations of the system, i.e., Eq (5.1). Figure 7(a) shows the largest Lyapunov exponent convergence with time indicating the stability and precision of the numerical integration process. The gradual approach to a positive value of the maximum eigenvalue of the system shows a steady estimate of the chaotic behavior. The change of the maximal eigenvalue, as a function of the parameter, Q, is shown in Figure 7(b). The largest Lyapunov exponent λ_{max} declines sharply with the growing values of Q. This dynamical behavior shows that the system switches between a strongly chaotic state to a weakly chaotic or close-to-stable state. These findings give a quantitative standard with regard to the phase portrait and the bifurcation analyses. We also computed the L_2 error norm between analytical and numerical profiles in order to determine the accuracy, where the small value ($E_{L_2} = 1.3 \times 10^{-4}$) was obtained that indicates the numerical consistency, and stability of the solutions obtained.

7. Results and discussion

Here, we will study dynamical behavior of the discussed fractional-order nonlinear system analytically and numerically. We use a wave transformation and the generalized Riccati-Bernoulli sub-ODE method and Bäcklund transformation to analytically solve and examine the qualitative nature of the solutions by creating phase portraits, time series plots, and energy density surfaces. The consequences of changing the fractional-order parameter (α) are discussed with the emphasis on the transition between the classical and fractional regimes and on the implications that this change has on the structure, stability, and localization of the solutions. With the addition of the conformable fractional derivative, this adds a nonlocal time dependence to the system, that is, the current state of the wave is dependent on its past behavior. The smaller the fractional-order (α), the greater the effective memory of the system which is a hereditary effect in the magneto-electro-elastic medium. This scaling parameter (α) is used to adjust the energy dissipation and dispersion rate, allowing a smooth transition between pure elastic regimes ($\alpha = 1$) and memory-driven regimes ($0 < \alpha < 1$). Therefore, the amplitude and width of solitons in terms of (α) are quantitatively used to explain the memory-dependent behavior of that medium.

Figure 1 shows the integer-order 3D depiction, as well as the fractional-order variations, 2D profiles of the solution at different values of (α), and their respective contour plots. A dark kink soliton emerges in a classical case, depicted in the 3D plot by a sharp, universally localized transition between two stable states. The structure is also stable and in accordance with the non-dispersive, coherent solution. As (α) is reduced in the 2D fractional plots, a wider and smoother soliton profile is observed which represents the role of memory and hereditary effects brought in by the conformable fractional derivative. These transitions are also demonstrated in contour plots where we realize the

spread and localization of the solution in space-time. These visualizations validate that the fractional-order parameter is important in dictating the amplitude, sharpness, and localization of waves which are critical aspects in modeling real-world nonlinear media like optical fibers, viscoelastic materials, and biological tissues.

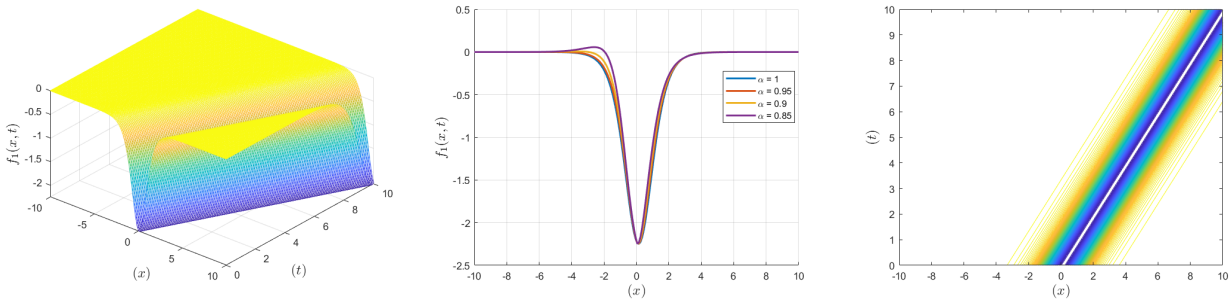

(a) **(b)** **(c)**

Figure 1. Graphical representations of the solution $f_1(x,t)$ for various fractional-order parameter (α). (a) 3D wave profile for integer-order ($\alpha = 1$), (b) 2D plot for fractional-order parameter ($\alpha = 1, 0.95, 0.90, 0.85$), and (c) the corresponding contour map, with parameters $Q = 1.0, v = 1.0, \omega = 0.5, k_1 = 0.3, k_2 = 0.02$.

Figure 2 shows the lump-type kink solution profile. The 3D plot is the integer-order plot, where there is a smooth and local object wave structure that implies a stable transition in space-time. In this combination, the 2D plots demonstrate how the fractional-order parameter (α) changes the effect, and the contour plot reveals how the energy gets localized and spread. The larger the fractional-order, the more the kink is perturbed with respect to the classical case that possesses sharper transitions and is steeper. Such an action is symptomatic of the nonlocal and memory-dependent effects that the conformable fractional derivative brings. This kind of sensitivity indicates the versatility of the fractional framework when detecting richer and more complicated wave dynamics, and they have the promise of applicability in nonlinear optics, fluid flow, and in signal transmission in complex media.

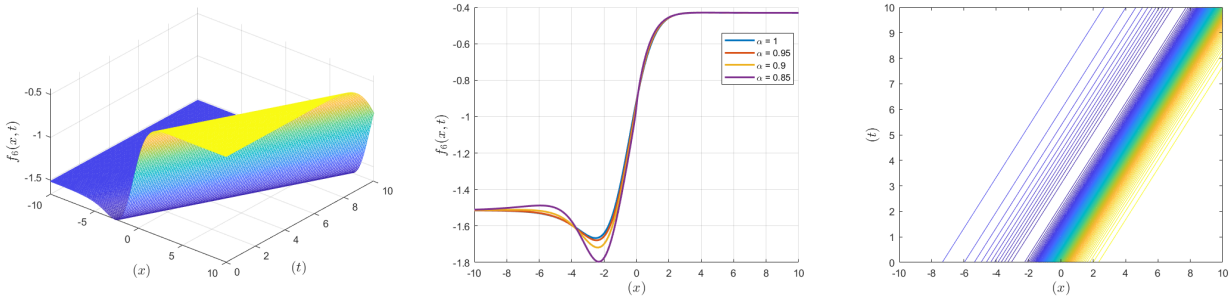

(a) **(b)** **(c)**

Figure 2. Graphical representations of the solution $f_6(x,t)$ for various fractional-order parameter (α). (a) 3D wave profile for integer-order ($\alpha = 1$), (b) 2D plot for fractional-order parameter ($\alpha = 1, 0.95, 0.90, 0.85$), and (c) the corresponding contour map, with parameters $Q = 1.0, v = 1.0, \omega = 0.5, k_1 = 0.3, k_2 = 0.02$.

Figure 3 depicts the dynamics of a dark kink soliton. The integer-order case in the 3D plot has a stable and localized transition, which agrees with classical soliton behavior. The 2D plots show the development of the solution with the consumption of various fractional-order solutions of (α). As the values of (α) are raised, the amplitude of the solution is more effective in the case of the fractional derivative compared to the integer-order case, an aspect that shows an increasing effect of the fractional derivative on the wave profile. This implies that the wave interaction and concentration of energy increase with the order of fractions and allow more control of solitons' amplitude and point in the nonlinear systems. The results are of particular interest to applications that deal with energy transport, nonlinear signal processing, and materials that have memory effects.

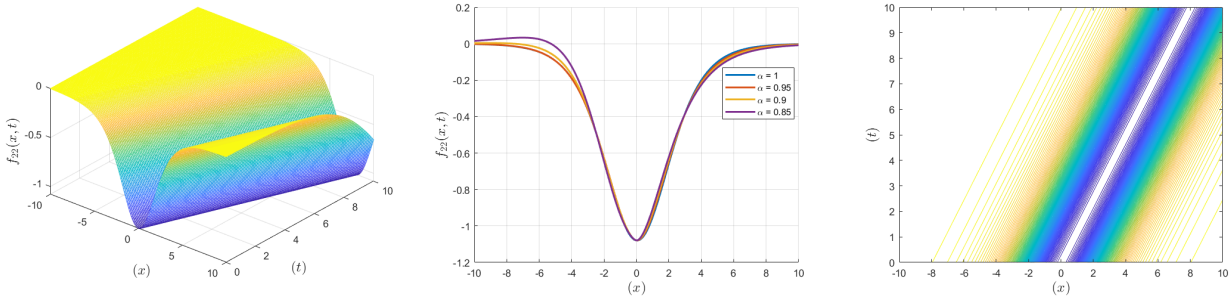

(a) **(b)** **(c)**

Figure 3. Graphical representations of the solution $f_{22}(x,t)$ for various fractional-order parameter (α). (a) 3D wave profile for integer-order ($\alpha = 1$), (b) 2D plot for fractional-order parameter ($\alpha = 1, 0.95, 0.90, 0.85$), and (c) the corresponding contour map, with parameters $Q = 1.0, v = 1.0, \omega = 0.5, L = 0.01, M = 0.8, k_1 = 0.3, k_2 = 0.02$.

Figure 4 has a similar structure of a dark kink soliton as in the case of Figure 3. The integer-order case is replicated in a symmetric and stable localized wave in the 3D plot. A marked difference in the 2D plots of different fraction-order values (α) is shown, as the wave is localized asymmetrically. In particular, the solution has the form of localization at one end and an increase in amplitude on the other, which is absent under the classical situation. This asymmetry shows the sensitivity of direction and the nonlocal effect, which is brought about by the conformable fractional derivative. That kind of behavior can be used to model anisotropic or direction biased media, providing important data when attempting applications to inhomogeneous/layered media, biophysical transport in complex materials, and asymmetric energy systems where the use of direction biased media is physically relevant.

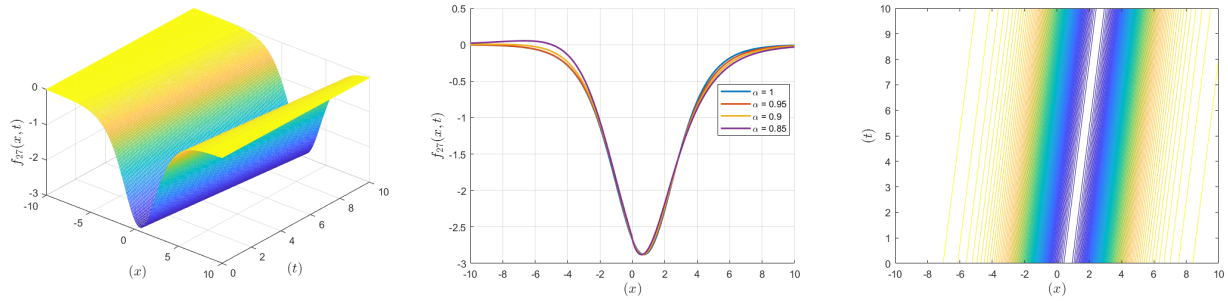

(a) **(b)** **(c)**

Figure 4. Graphical representations of the solution $f_1(x,t)$ for various fractional-order parameter (α). (a) 3D wave profile for integer-order ($\alpha = 1$), (b) 2D plot for fractional-order parameter ($\alpha = 1, 0.95, 0.90, 0.85$), and (c) the corresponding contour map, with parameters $Q = 1.0, v = 1.0, \omega = 0.5, k_1 = 0.3, k_2 = 0.02$.

Figure 5 shows the phase portrait of the system in the (y, g) plane, where $y(\wp)$ is the main dynamical variable and $g(\wp)$ is its conformable fractional derivative. A center type equilibrium at the origin of the plot $(0, 0)$ shows clearly in this trajectory graph as would a nonlinear oscillator experiencing bounded periodic behavior. Nevertheless, the system, at resistance to the fractional-order influence, shows localized structures on one of the sides of the phase space, with amplitude increasing on the other. The conformable fractional derivative associated with this asymmetry is a natural property of the direction in which it has memory effects. The resulting trajectory is a non-symmetric closed loop, implying quasi-periodicity and a non-conservative characteristic of the traditional integer-order systems. The symmetry of the dynamics becomes more apparent after we consider the plots of the time series. In the top panel, we can see $y(\wp)$ varying at a fairly constant frequency with increasing amplitude from one side to the other. This conforms to what is observed in the phase portrait: a wave is concentrated on one side with this fractional influence resulting in amplification of the wave as $(\wp)$ increases. The derivative $g(\wp)$, corresponding to the bottom panel, also has damped oscillations. Such a tendency recently created is indicative of the loss of symmetry and a mild redistribution of energy within the system as it evolves through time which, of course, is an anticipated outcome of fractional-order damping-like influences that would not occur in the integer-order case. Altogether, the time series proves the directional modulation caused by the fractional-order.

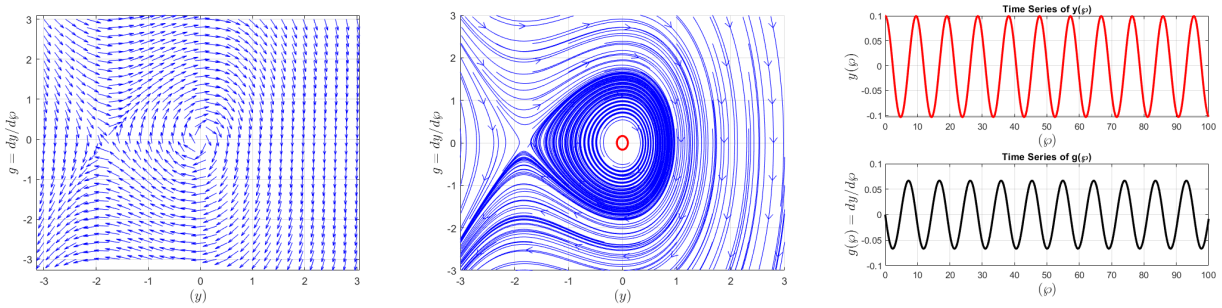

(a) **(b)** **(c)**

Figure 5. Time series plot of Eq (5.1) with initial conditions (0.1, 0), and phase portrait plots of Eq (4.3), depicting the dynamical behavior of the system under study.

To provide a clearer insight of the energetic dynamics of the system, Figure 6 depicts the Hamiltonian energy surface $H(y, g)$, which is formed using the Hamiltonian-derived function including y and its associated conjugate momentum g. The surface of energy has non-trivial topology and is smoothly undulating with several saddle-like areas, in which energy density is accumulated or dispersed. This 3D surface enables us to see how the overall energy of the system varies when the state variables are varied. The peaks and troughs stand in plausible regions of localization or transition and the asymmetry in the curvature is representative of the non-conservative nature of the fractional system. It is worth mentioning that the appearance of the two valleys indicates multi-stable energy states in favor of the existence of quasi-periodic structures which have a soliton-like nature.

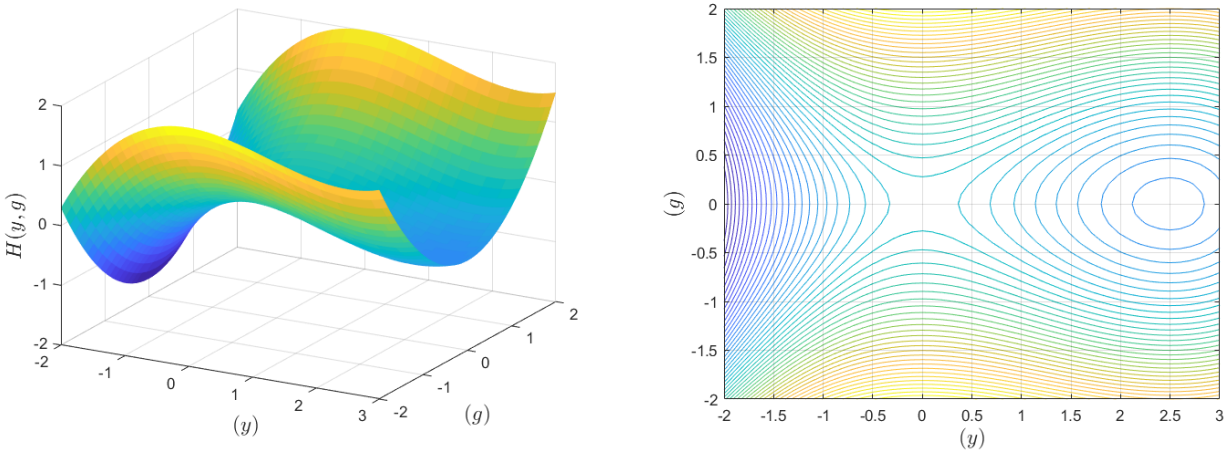

(a) **(b)**

Figure 6. Energy density plot of Eq (4.4), illustrating the distribution and evolution of energy in the system.

Besides the representative cases in Figure 7, there is also a richness of nonlinear wave behavior in the rest of the analytical solutions. These are localized, oscillatory, and kink-type structures that elucidate smooth transitions, periodic modulations, or solitary pulses that rely on the physical parameters and the fractional-order index. Taken together, the above solutions can deepen the

qualitative insights into the dynamics of the system and underscore the sensitivity of nonlinear wave profiles in the fractional derivative to changes in the fractional derivative of nonlinear media of complex nonlinearity and memory.

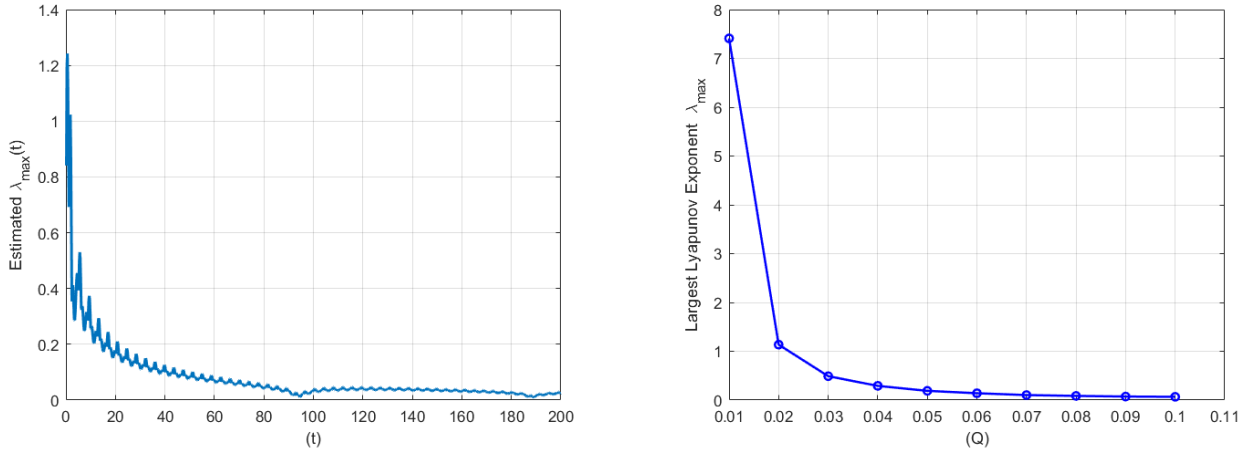

(a) **(b)**

Figure 7. The first plot shows stable convergence of λ_{max} over time, confirming numerical accuracy, while the second plot illustrates its variation against Q, marking the transition from regular to chaotic dynamics.

In order to give a more systematic view of the effect of system parameters, Figure 8 shows the behavior of the fractional solutions $f_6(x,t)$ and $f_{27}(x,t)$ with various values of the wave and material constants. In more detail, the behavior of $f_6(x,t)$ with respect to frequency ω variations and that of $f_{27}(x,t)$ with respect to dispersion constant Q and wave velocity v are investigated. The findings show that an increase in ω increases the frequency and compression of waves, and changes in Q and v considerably alter the amplitude, width, and propagation of the nonlinear wave. These results underline the sensitivity of the proposed fractional MEE system to significant physical parameters and present it as effective in the representation of complex dispersive behaviors.

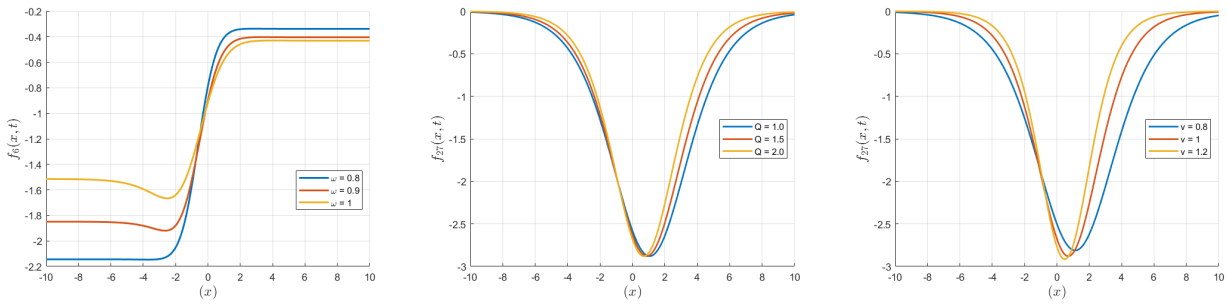

(a) **(b)** **(c)**

Figure 8. Parameters on the fractional wave profile: (a) variation of $f_6(x,t)$ with frequency ω, (b) variation of $f_{27}(x,t)$ with dispersion constant Q, and (c) variation of $f_{27}(x,t)$ with wave velocity v for fixed fractional-order $\alpha = 1$.

8. Conclusions

In our study we have investigated a nonlinear dynamical system whose description is based upon a conformable fractional-order derivative framework. Using a wave transformation and the generalized Riccati-Bernoulli sub-ODE method with the Bäcklund transformation, we were able to arrive at various, exact analytical soliton solutions. The fractional-order permitted the representation of complicated behaviors, which are unavailable in traditional integer-order systems.

Study of the phase portraits showed the presence of asymmetric periodic orbits and non-central equilibria, which confirm that the fractional derivative has directional effects that were imposed. Time series depictions supported the start of one-sided localization, which became more pronounced with increasing amplitudes and modulated oscillations, typical of quasi-periodic motions.

In order to supplement the analysis carried out in the phase space we designed the associated Hamiltonian function and generated the energy density surface. The resulting topology of the landscape was very rich and had a variety of energetic basins and saddle points, which indicate that there exist multi-stable dynamical regimes. This emphasizes the proposed system's ability to generate localized solutions and the involved wave interactions.

In general, our findings highlight the potential of conformable fractional calculus to enable realistic and complex dynamical behavior, including energy asymmetry, non-conservative dynamics, and direction-dependent evolution. Not only do these results contribute to a theoretical understanding of fractional nonlinear systems, but also open up the potential use of these results in applications where nonlocal interactions and memory are essential, e.g., nonlinear acoustics, hydrodynamics, and optical media. Regarding future directions, we can analyze the stability of the solutions acquired by the above method, the impact of additional changes in the value of fractional-order parameter (α), and the implementation of it to higher dimensional or coupled systems, thus expanding the dimension of the fractional theory of nonlinear waves.

Use of Generative-AI tools declaration

The author declares he has not used Artificial Intelligence (AI) tools in the creation of this article.

Acknowledgments

The author extends his appreciation to Taif University, Saudi Arabia, for supporting this work through project number (TU-DSPP-2025-66).

Funding

This research was funded by Taif University, Saudi Arabia, Project No. (TU-DSPP-2025-66).

Conflict of interest

The author declares that he has no conflict of interest.

References

1. M. Vinyas, Computational analysis of smart magneto-electro-elastic materials and structures: Review and classification, *Arch. Comput. Methods Eng.*, **28** (2021), 1205–1248. http://dx.doi.org/10.1007/s11831-020-09406-4
2. B. L. Wang, Y. W. Mai, Applicability of the crack-face electromagnetic boundary conditions for fracture of magneto-electro-elastic materials, *Int. J. Solids Struct.*, **44** (2007), 387–398. http://dx.doi.org/10.1016/j.ijsolstr.2006.04.028
3. Y. Sui, W. Wang, H. Zhang, Effects of electromagnetic fields on the contact of magneto-electro-elastic materials, *Int. J. Mech. Sci.*, **223** (2022), 107283. http://dx.doi.org/10.1016/j.ijmecsci.2022.107283
4. M. A. Koc, I. Esen, M. Eroglu, Thermo-mechanical vibration response of nano-plates with magneto-electro-elastic face layers and functionally graded porous core using nonlocal strain gradient elasticity, *Mech. Adv. Mater. Struct.*, **31** (2024), 4477–4509. http://dx.doi.org/10.1080/15376494.2023.2199412
5. X, Li, P, Gao, W. Liu, Geometric-stair-shaped super-regular breathers induced by PT-symmetric nonlinearity, *Phys. Rev. A*, **111** (2025), 033515. http://dx.doi.org/ 10.1103/PhysRevA.111.033515
6. A. A. Alderremy, S. Aly, R. Fayyaz, A. Khan, R. Shah, N. Wyal, The analysis of fractional-order nonlinear systems of third order KdV and Burgers equations via a novel transform, *Complexity*, **2022** (2022), 4935809. http://dx.doi.org/ 10.1155/2022/4935809
7. E. M. Elsayed, R. Shah, K. Nonlaopon, The analysis of the fractional-order Navier-Stokes equations by a novel approach, *J. Funct. Space*, **2022** (2022), 8979447. http://dx.doi.org/ 10.1155/2022/8979447
8. M. Naeem, H. Rezazadeh, A. A. Khammash, S. Zaland, Analysis of the fuzzy fractional-order solitary wave solutions for the KdV equation in the sense of Caputo-Fabrizio derivative, *J. Math.*, **2022** (2022), 3688916. http://dx.doi.org/ 10.1155/2022/3688916
9. M. Alqhtani, K. M., Saad, W. M. Hamanah, Discovering novel soliton solutions for (3+1)-modified fractional Zakharov-Kuznetsov equation in electrical engineering through an analytical approach, *Opt. Quant. Electron.*, **55** (2023), 1149. http://dx.doi.org/10.1007/s11082-024-06763-3
10. H. Yasmin, A. S. Alshehry, A. H. Ganie, A. Shafee, Noise effect on soliton phenomena in fractional stochastic Kraenkel-Manna-Merle system arising in ferromagnetic materials, *Sci. Rep.*, **14** (2024), 1810. http://dx.doi.org/10.1038/s41598-024-52211-3
11. H. Rezazadeh, H. Tariq, M. Eslami, M. Mirzazadeh, Q. Zhou, New exact solutions of nonlinear conformable time-fractional Phi-4 equation, *Chin. J. Phys.*, **56** (2018), 2805–2816. http://dx.doi.org/10.1016/j.cjph.2018.08.001
12. A. K. Alsharidi, A. Bekir, Discovery of new exact wave solutions to the M-fractional complex three coupled Maccari's system by Sardar sub-equation scheme, *Symmetry*, **15** (2023), 1567. http://dx.doi.org/10.3390/sym15081567
13. K. Faisal, S. Abbagari, A. Pashrashid, A. Houwe, S. W. Yao, H. Ahmad, Pure-cubic optical solitons to the Schrodinger equation with three forms of nonlinearities by Sardar sub-equation method, *Results Phys.*, **48** (2023), 106412. http://dx.doi.org/10.1016/j.rinp.2023.106412

14. Y. Asghari, M. Eslami, H. Rezazadeh, Exact solutions to the conformable time-fractional discretized mKdV lattice system using the fractional transformation method, *Opt. Quant. Electron.*, **55** (2023), 318. http://dx.doi.org/10.1007/s11082-022-04529-3

15. B. Hong, Exact solutions for the conformable fractional coupled nonlinear Schrodinger equations with variable coefficients, *J. Low Freq. Noise Vib. Act. Control*, **42** (2023), 628–641. https://doi.org/10.1177/14613484221135478

16. Q. Yin, B. Gao, Z. Shi, Distinct exact solutions for the conformable fractional derivative Gerdjikov-Ivanov equation via three credible methods, *J. Taibah Univ. Sci.*, **17** (2023), 2251219. https://doi.org/10.1080/16583655.2023.2251219

17. H. Ahmad, M. N. Alam, M. A. Rahman, M. F. Alotaibi, M. Omri, The unified technique for the nonlinear time-fractional model with the beta derivative, *Results Phys.*, **29** (2021), 104785. http://dx.doi.org/10.1016/j.rinp.2021.104785

18. M. S. Ullah, H. O. Roshid, M. Z. Ali, New wave behaviors of the Fokas-Lenells model using three integration techniques, *PloS One*, **18** (2023), e0291071. http://dx.doi.org/10.1371/journal.pone.0291071

19. M. S. Ullah, M. Mostafa, M. Z. Ali, H. O. Roshid, M. Akter, Soliton solutions for the Zoomeron model applying three analytical techniques, *PloS One*, **18** (2023), e0283594. http://dx.doi.org/10.1371/journal.pone.0283594

20. M. N. Alam, S. M. R. Islam, The agreement between novel exact and numerical solutions of nonlinear models, *Partial Differ. Equ. Appl. Math.*, **8** (2023), 100584. http://dx.doi.org/10.1016/j.padiff.2023.100584

21. M. Alqhtani, K. M. Saad, R. Shah, W. Weera, W. M. Hamanah, Analysis of the fractional-order local Poisson equation in fractal porous media, *Symmetry*, **14** (2022), 1323. http://dx.doi.org/10.3390/sym14071323

22. R. Shah, Y. Alkhezi, K. Alhamad, An analytical approach to solve the fractional Benney equation using the q-homotopy analysis transform method, *Symmetry*, **15** (2023), 669. http://dx.doi.org/10.3390/sym15030669

23. S. Noor, A. S. Alshehry, A. Shafee, R. Shah, Families of propagating soliton solutions for (3+1)-fractional Wazwaz-BenjaminBona-Mahony equation through a novel modification of modified extended direct algebraic method, *Phys. Scr.*, **99** (2024), 045230. http://dx.doi.org/ 10.1088/1402-4896/ad23b0

24. R. Shah, A. Saad Alshehry, W. Weera, A semi-analytical method to investigate fractional-order gas dynamics equations by Shehu transform. *Symmetry*, **14** (2022), 1458. http://dx.doi.org/10.3390/sym14071458

25. A. S. Alshehry, H. Yasmin, F. Ghani, R. Shah, K. Nonlaopon, Comparative analysis of advection-dispersion equations with Atangana-Baleanu fractional derivative, *Symmetry*, **15** (2023), 819. http://dx.doi.org/ 10.3390/sym15040819

26. K. Wang, An effective computational approach to the local fractional low-pass electrical transmission lines model, *Alex. Eng. J.*, **110** (2025), 629–635. http://dx.doi.org/10.1016/j.aej.2024.07.021

27. K. Yang, A unified solution for longitudinal wave propagation in an elastic rod, *J. Sound Vib.*, **314** (2008), 307–329. http://dx.doi.org/10.1016/j.jsv.2008.01.007
28. M. N. Alam, C. Tunc, Construction of soliton and multiple soliton solutions to the longitudinal wave motion equation in a magneto-electro-elastic circular rod and the Drinfeld-Sokolov-Wilson equation, *Miskolc Math. Notes*, **21** (2020), 545–561. http://dx.doi.org/ 10.18514/MMN.2020.3138
29. B. K. Singh, S. Agrawal, A new approximation of conformable time fractional partial differential equations with proportional delay, *Appl. Numer. Math.*, **157** (2020), 419–433. http://dx.doi.org/10.1016/j.apnum.2020.07.001
30. A. R. Seadawy, J. Manafian, New soliton solution to the longitudinal wave equation in a magneto-electro-elastic circular rod, *Results Phys.*, **8** (2018), 1158–1167. http://dx.doi.org/10.1016/j.rinp.2018.01.062
31. H. Durur, A. Yokus, D. Kaya, H. Ahmad, Modeling of dark solitons for nonlinear longitudinal wave equation in a magneto-electro-elastic circular rod, *Sound Vib.*, **55** (2021), 241–251. http://dx.doi.org/10.32604/sv.2021.014157
32. M. S. Islam, M. A. Akbar, K. Khan, The improved F-expansion method and its application to the MEE circular rod equation and the ZKBBM equation, *Cogent Math.*, **4** (2017), 1378530. http://dx.doi.org/10.1080/23311835.2017.1378530
33. M. Iqbal, A. R. Seadawy, D. Lu, Applications of nonlinear longitudinal wave equation in a magneto-electro-elastic circular rod and new solitary wave solutions, *Mod. Phys. Lett. B*, **33** (2019), 1950210. http://dx.doi.org/10.1142/S0217984919502105
34. H. M. Baskonus, H. Bulut, A. Atangana, On the complex and hyperbolic structures of the longitudinal wave equation in a magneto-electro-elastic circular rod, *Smart Mater. Struct.*, **25** (2016), 035022. http://dx.doi.org/10.1088/0964-1726/25/3/035022
35. N. Sajid, G. Akram, Solitary dynamics of longitudinal wave equation arises in magneto-electro-elastic circular rod, *Mod. Phys. Lett. B*, **35** (2021), 2150086. http://dx.doi.org/10.1142/S021798492150086X
36. C. X. Xue, E. Pan, S. Y. Zhang, Solitary waves in a magneto-electro-elastic circular rod, *Smart Mater. Struct.*, **20** (2011), 105010. http://dx.doi.org/10.1088/0964-1726/20/10/105010
37. N. H. Aljahdaly, R. G. ALoufi, A. R. Seadawy, Stability analysis and soliton solutions for the longitudinal wave equation in magneto electro-elastic circular rod, *Results Phys.*, **26** (2021), 104329. https://doi.org/10.1016/j.rinp.2021.104329
38. F. S. Khodadad, F. Nazari, M. Eslami, H. Rezazadeh, Soliton solutions of the conformable fractional Zakharov-Kuznetsov equation with dual-power law nonlinearity, *Opt. Quant. Electron.*, **49** (2017), 384. http://dx.doi.org/10.1007/s11082-017-1225-y
39. E. M. E. Zayed, K. A. E. Alurrfi, The Bäcklund transformation of the Riccati equation and its applications to the generalized KdV-mKdV equation with any-order nonlinear terms, *Pan-Am. Math. J.*, **26** (2016), 50–62.